0022-3565/02/3033-1067–1074$7.00
THE JOURNAL OF PHARMACOLOGY AND EXPERIMENTAL THERAPEUTICS
JPET 303:1067–1074, 2002

Vol. 303, No. 3
38570/1026540
Printed in U.S.A.

The Sea Anemone Toxins BgII and BgIII Prolong the Inactivation Time Course of the Tetrodotoxin-Sensitive Sodium Current in Rat Dorsal Root Ganglion Neurons

EMILIO SALCEDA, ANOLAND GARATEIX, and ENRIQUE SOTO

Instituto de Fisiología, Universidad Autónoma de Puebla, México (Em.S., En.S.); and Instituto de Oceanología, Ministerio de Ciencia, Tecnologia y Medio Ambieute, La Habana, Cuba (A.G.)

Received May 23, 2002; accepted September 4, 2002

ABSTRACT

We have characterized the effects of BgII and BgIII, two sea anemone peptides with almost identical sequences (they only differ by a single amino acid), on neuronal sodium currents using the whole-cell patch-clamp technique. Neurons of dorsal root ganglia of Wistar rats (P5-9) in primary culture (Leibovitz's L15 medium; 37°C, 95% air/5% CO_2) were used for this study ($n = 154$). These cells express two sodium current subtypes: tetrodotoxin-sensitive (TTX-S; $K_i = 0.3$ nM) and tetrodotoxin-resistant (TTX-R; $K_i = 100$ μM). Neither BgII nor BgIII had significant effects on TTX-R sodium current. Both BgII and BgIII produced a concentration-dependent slowing of the TTX-S sodium current inactivation ($IC_{50} = 4.1 \pm 1.2$ and 11.9 ± 1.4 μM, respectively), with no significant effects on activation time course or current peak amplitude. For comparison, the concentration-dependent action of *Anemonia sulcata* toxin II (ATX-II), a well characterized anemone toxin, on the TTX-S current was also studied. ATX-II also produced a slowing of the TTX-S sodium current inactivation, with an IC_{50} value of 9.6 ± 1.2 μM indicating that BgII was 2.3 times more potent than ATX-II and 2.9 times more potent than BgIII in decreasing the inactivation time constant (τ_h) of the sodium current in dorsal root ganglion neurons. The action of BgIII was voltage-dependent, with significant effects at voltages below −10 mV. Our results suggest that BgII and BgIII affect voltage-gated sodium channels in a similar fashion to other sea anemone toxins and α-scorpion toxins.

Voltage-dependent sodium channels have receptor sites that may be recognized by different groups of neurotoxins (Adams and Olivera, 1994; Trainer et al., 1994). For this reason, this kind of compound has been shown to be a useful pharmacological tool for studying the functional and structural mapping of sodium channel proteins (Catterall, 2000). Toxins that act on sodium channels can be classified in two main groups according to their pharmacological effects on the channel: blockers (e.g., tetrodotoxin and μ-conotoxin) and modulators (e.g., batrachotoxin, α- and β-scorpion toxins, and sea anemone toxins). The latter is further divided into several classes based upon the effects on channel activation and inactivation kinetics (Narahashi, 1998).

A large number of neurotoxins have modulatory actions on Na^+ channel function by modifying the processes linked to channel activation and inactivation, ionic selectivity, and other properties involved in action potential generation. At least six neurotoxin receptor sites have been identified on the mammalian sodium channel (Strichartz et al., 1987; Catterall, 1995). Anemone peptide neurotoxins and α-scorpion toxins share receptor site 3 on sodium channels (Couroud et al., 1978; Catterall, 1995, 2000; Gordon et al., 1998), which involves the extracellular loops IS5-S6, IVS3-S4, and IVS5-S6 of the ionic channel (Rogers et al., 1996). Anemone toxins are generally smaller than the structurally unrelated α-scorpion toxins and have three rather than four disulfide bridges (Norton, 1997); nevertheless, both groups bind to site 3, exhibit similar pharmacological properties, displace one another from their binding site, and their main effect is to delay channel inactivation, resulting in a prolongation of the action potential.

Bunodosoma granulifera is an anemone species very common at the Cuban seashores. Several active compounds with pharmacological actions on ionic channels have been isolated from its secretions (Aneiros et al., 1993; Loret et al., 1994; Dauplais et al., 1997; Salinas et al., 1997; Alessandri-Haber et al., 1999; Garateix et al., 2000). Among them, BgII and BgIII are two peptide toxins (molecular masses: 5072 and 5073, respectively) with almost identical sequences (they only differ by a single amino acid), causing toxicity in mice

This work was supported by CONACyT Grant E120.1869/2000
Article, publication date, and citation information can be found at http://jpet.aspetjournals.org.
DOI: 10.1124/jpet.102.038570.

ABBREVIATIONS: DRG, dorsal root ganglion; TTX-S, tetrodotoxin-sensitive; TTX-R, tetrodotoxin-resistant; L15, Leibovitz's L15 medium; τ_h, inactivation time constant; ATX-II, *Anemonia sulcata* toxin II; G_{Na}, peak sodium conductance.

when injected intracerebroventricularly and markedly different binding to rat brain synaptosomes; both effects are higher for BgII (Loret et al., 1994).

In this work, we have characterized the effects of BgII and BgIII toxins on neuronal sodium currents. Rat dorsal root ganglion (DRG) neurons were chosen for this study since these cells express two sodium current subtypes: a tetrodotoxin-sensitive (TTX-S) sodium current, which is readily blocked by TTX (K_I = 0.3 nM), and a tetrodotoxin-resistant (TTX-R) sodium current, which is highly resistant to TTX (K_i = 100 μM) (Roy and Narahashi, 1992; Novakovik et al., 2001). To our knowledge, this is the first electrophysiological characterization of the action of these toxins on neuronal cells.

Materials and Methods

Animal care and procedures were carried out in accordance with the Declaration of Helsinki. The number of animals used for this work was kept to the minimum necessary for a meaningful interpretation of the data.

Toxins. BgII and BgIII were isolated and purified from sea anemone *B. granulifera*, as previously described (Aneiros et al., 1993; Loret et al., 1994). Some experiments were performed with ATX-II obtained from the sea anemone *Anemonia sulcata* (a gift from Professor L. Beress, Kiel, Germany). TTX was obtained from Sigma-Aldrich (St. Louis, MO). Aliquots of stock solution in deionized water were prepared and stored in a freezer (−20°C). Before each experiment, they were dissolved in the perfusion solution.

Cell Preparation. Young Wistar rats (P5-9) of either sex were anesthetized with ether and subsequently decapitated. DRGs were isolated from the vertebral column and incubated (30 min at 37°C) in Leibovitz's L15 medium (L15) (Invitrogen, Carlsbad, CA) containing 1.125 mg/ml trypsin and 1.125 mg/ml collagenase (both from Sigma-Aldrich). Following enzyme treatment, the ganglia were washed 3 times with sterile L15 and mechanically dissociated. The cells were then plated onto 35-mm culture dishes (Corning, Corning, NY) containing 12 × 10-mm glass coverslips (Corning) previously coated with poly-D-lysine (Sigma-Aldrich). Neurons were incubated 4 to 6 h in a humidified atmosphere (95% air/5% CO_2 at 37°C, using a CO_2 water-jacketed incubator; Nuaire, Plymouth, MN) to allow the isolated cells to settle and adhere to the coverslips. The incubation medium (pH 7.4) contained L15, 15.7 mM $NaHCO_3$ (Merck, Naucalpan, Mexico), 10% fetal bovine serum, 2.5 μg/ml Fungizone (both from Invitrogen), 100 U/ml penicillin (Lakeside, Toluca, Mexico), and 15.8 mM HEPES (Sigma-Aldrich).

Electrophysiological Recording. A coverslip with attached neurons was transferred to a 500-μl perfusion chamber mounted on the stage of an inverted phase-contrast microscope (Nikon Diaphot, Tokyo, Japan). Cells were bathed with an external solution containing 20 mM NaCl, 1 mM $MgCl_2$, 1.8 mM $CaCl_2$, 45 mM TEA-Cl, 70 mM choline chloride, 10 mM 4-aminopyridine, and 5 mM HEPES. The pH of this solution was adjusted to 7.4 with HCl. Osmolarity was monitored by a vapor pressure osmometer (Wescor, Logan, UT) and adjusted to 290 mOsm using dextrose. A gravity-driven perfusion system maintained the external solution flowing into the chamber at a rate of around 100 μl/min. In addition to this perfusion system, a double-barrel array built up with borosilicate glass capillaries (TW120–3; WPI, Sarasota, FL) was placed approximately 40 μm above the cell under study; each barrel was coupled to an independent syringe driven by a Baby Bee pump (BAS, West Lafayette, IN). Through this system, the neuron was continuously microperfused (10 μl/min) with external solution or with external solution plus toxin. Some experiments were designed to study the effects of BgII or BgIII on TTX-R sodium currents. To achieve this, TTX (300 nM) was added to both bath and microperfusion solutions.

The whole-cell patch-clamp technique was used to record ionic currents. Patch pipettes were pulled from borosilicate glass capillaries (TW120–3; WPI), using a Flaming-Brown electrode puller (P80/PC; Sutter Instruments, San Rafael, CA), which had resistances of 0.9 to 1.8 MΩ when filled with internal solution. Pipette solution contained 10 mM NaCl, 100 mM CsF, 30 mM CsCl, 10 mM TEA-Cl, 8 mM EGTA, and 5 mM HEPES. The pH of this solution was adjusted to 7.3 with CsOH. Osmolarity was adjusted to 300 mOsm. The internal solution was filtered on the day of use with a 0.22-μm pore size syringe filter (Millipore, Bedford, MA).

To measure ionic currents, an Axopatch-1D amplifier (Axon Instruments, Foster City, CA) was used. Command pulse generation and data sampling were controlled by the PClamp 8.0 software (Axon Instruments) using a 16-bit data acquisition system (Digidata 1320A; Axon Instruments). Signals were low-pass filtered at 5 kHz and digitized at 20 kHz. Leakage and capacitive currents were digitally subtracted with the P-P/2 method. Capacitance and series resistance (80%) were electronically compensated. Experiments were rejected when, at the maximum peak current, the voltage error exceeded 5 mV after compensation of series resistance. No corrections were made for smaller values.

The type of sodium current present in the cell under study was determined before each experiment. In accordance with the criterion used by Strachan et al. (1999), only those cells with <10% TTX-R sodium current, as derived from a steady-state inactivation profile, were accepted to determine the effects of BgII and BgIII on TTX-S sodium currents. Experiments were performed at room temperature (23–25°C).

Data Analysis. Recordings were analyzed off-line using PClamp 8.0 and Origin software (Microcal Software, Northampton, MA). Statistical differences were determined using a Student's t test with $p < 0.05$. Curve-fitting routines were performed using a nonlinear least-squares method. Numerical data are presented as the mean ± S.E. for at least four measurements.

Concentration-response curves were obtained by measuring the parameters under study in sodium currents elicited by a single-step voltage protocol, where 40 ms depolarizing test pulses to −10 mV were applied from a holding potential of −90 mV every 8 s. Data were then plotted as a function of toxin concentration and fit by the following function.

$$y = A_1 + \frac{A_2 - A_1}{1 + 10^{(\log IC_{50} - x)\cdot P}}$$

where A_1 is the y value at the bottom plateau, A_2 is the y value at the top plateau, log IC_{50} is the x value when the response is halfway between A_1 and A_2, and P is the Hill slope.

To test whether BgII or BgIII showed a use-dependent action, from a holding potential of −90 mV repetitive pulses to −10 mV were applied at frequencies of 0.1, 1 and 5 Hz. Current-voltage relationships and availability curves were constructed using a standard double-pulse protocol; from a holding potential of −100 mV, a 40-ms test pulse to −10 mV was preceded by 40-ms prepulses between −100 and 70 mV (time interval between sweeps = 8 s).

The peak amplitudes of the currents were measured at the prepulse and converted to sodium conductance by means of the following equation:

$$G_{Na} = \frac{I_{Na}}{V_{test} - V_{rev}}$$

where G_{Na} is the sodium conductance, I_{Na} is the sodium current peak amplitude, V_{test} is the test potential, and V_{rev} is the reversal potential for the sodium current. Normalized conductance curves were then plotted and fit by a Boltzmann distribution with the following function.

$$\frac{G_{Na}}{G_{max}} = \frac{1}{1 + \exp\left(\frac{V_{test} - V_{1/2}}{k}\right)}$$

where G_{max} is the maximum sodium conductance, $V_{1/2}$ is the test potential that activates 50% of the sodium channels, k is the slope of the curve, and the other terms are as above.

The steady-state inactivation parameter (h_∞) was calculated by dividing the current achieved following a given prepulse by the maximum current achieved in the test pulse. The results of such operation were plotted as a function of the prepulse potential and were fitted by the following Boltzmann function.

$$h_\infty = \frac{1}{1 + \exp\left(\frac{V_{pre} - V_{1/2\ inact}}{k}\right)}$$

where V_{pre} is the prepulse potential, $V_{1/2\ inact}$ is the prepulse potential at which h_∞ is 0.5, and k is the slope of the curve at this mid-point.

The effects of BgII and BgIII on the rate at which sodium channels recover from inactivation were investigated using a two-pulse protocol with a variable interpulse interval (Δt) as follows: from a holding potential of −100 mV, a 40-ms conditioning prepulse to −10 mV was used to inactivate sodium channels, after which a 2.5-ms depolarizing test pulse to −10 mV was applied. The interpulse interval between the conditioning and the test pulses was varied between 1.25 and 80 ms. The peak current recorded during the test pulse was normalized against the current amplitude during the conditioning prepulse and plotted as a function of Δt. Data obtained from this protocol were fitted by a single exponential function.

Results

A total of 154 neurons (mean capacity = 52.5 ± 18 pF, S.D.) were successfully voltage-clamped for a sufficient time to allow the study of BgII, BgIII, and ATX-II actions. The capacitances of the DRG neurons used for this study formed a unimodal histogram with the mean, which corresponds to a cell diameter of about 41 μm. This distribution represents only the cells selected for recording, basically neurons with a medium size cell body (probably Aβ neurons).

The percentage of change in peak amplitude and activation and inactivation time constants were calculated for ionic currents from both TTX-S and -R sodium currents before and about 1 min after perfusion with toxin. For the TTX-S current subtype, concentration-response curves were obtained using concentrations of 0.1, 0.3, 1, 3, 10, and 30 μM. For the rest of the experiments in this study, we used a 10 μM toxin concentration.

To study the effects of BgII and BgIII on TTX-R sodium currents, TTX (300 nM) was added to both bath and microperfusion solutions (n = 15). This procedure made evident the existence of two subtypes of TTX-R current: 1) a slowly activating (τ = 0.46 ± 0.2 ms) and slowly inactivating (τ = 4.55 ± 1.96 ms) current that activates at about −40 mV (n = 7); and 2) a current that fails to inactivate, giving rise to a large late component (n = 8). These two types of TTX-R currents coincide with those previously described in DRG neurons (Bossu and Feltz, 1984; Baker and Wood, 2001). Neither 10 μM BgII (n = 9) nor 10 μM BgIII (n = 6) had significant effects ($p > 0.05$, Student's t test) on either TTX-R sodium current subtypes (Fig. 1).

Both BgII (n = 87) and BgIII (n = 22) produced a concentration-dependent effect on the TTX-S sodium current inactivation time course, with no significant effects ($p > 0.05$, Student's t test) on activation time course or current peak amplitude (Fig. 2). The inactivation time course of TTX-S sodium currents was adjusted with an exponential function over the following 10 ms after peak current. In the presence of 3 μM BgII, the inactivation time constant (τ_h) increased 97.6 ± 35.4%, whereas a 10 μM toxin concentration produced 154.2 ± 17.4% increase in τ_h. The IC_{50} value for BgII was 4.1 ± 1.2 μM, with a fixed slope value of 1.0. In contrast, the action of BgIII was less effective; at 3 μM, τ_h was increased 15.2 ± 8.5%, whereas at 10 μM, τ_h increased 60.9 ± 13.0%. The IC_{50} value for BgIII experiments was 11.9 ± 1.4 μM, with a fixed slope of 1.0.

To compare the effect of these toxins with ATX-II, a well

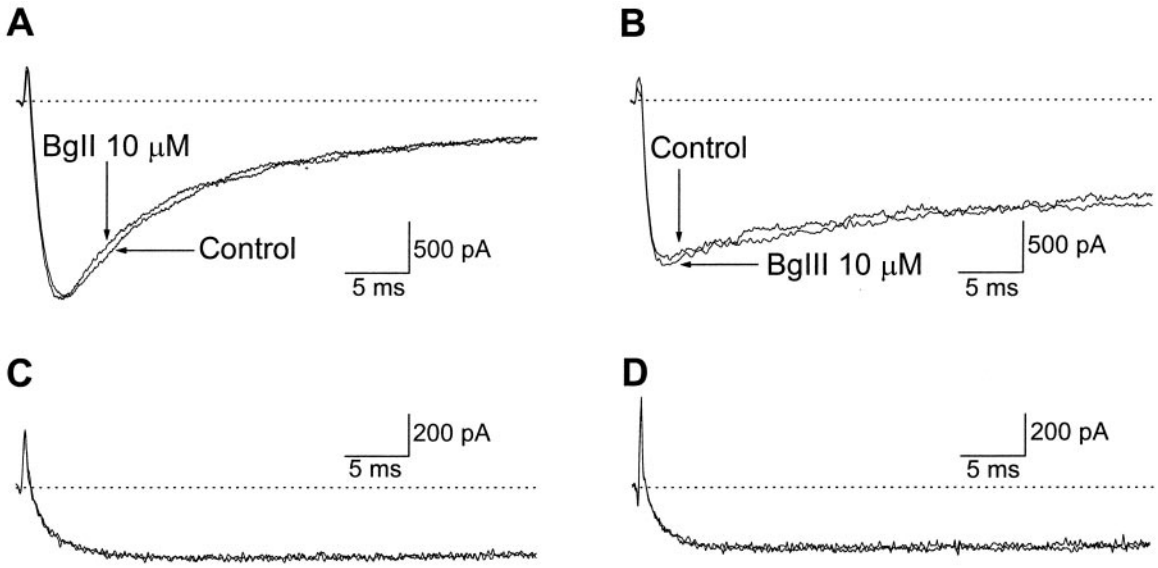

Fig. 1. Effects of 10 μM BgII (A and C) and BgIII (B and D) on TTX-R sodium currents (n = 15). Recordings were made in presence of 300 nM TTX. Currents were elicited by a single-step voltage protocol (40-ms depolarizing test pulses to −10 mV from a holding potential of −90 mV every 8 s). Two subtypes of TTX-R current were found, partially inactivating currents with a time constant τ = 4.55 ± 1.96 ms (A and B; n = 7) and very slow activating currents (τ = 1.38 ± 0.2 ms) failing to inactivate (C and D; n = 8). For each case, two superimposed traces are presented, under control conditions and approximately 2 min after toxin perfusion. Neither BgII (n = 9) nor BgIII (n = 6) produced significant effects on either TTX-R sodium current subtypes.

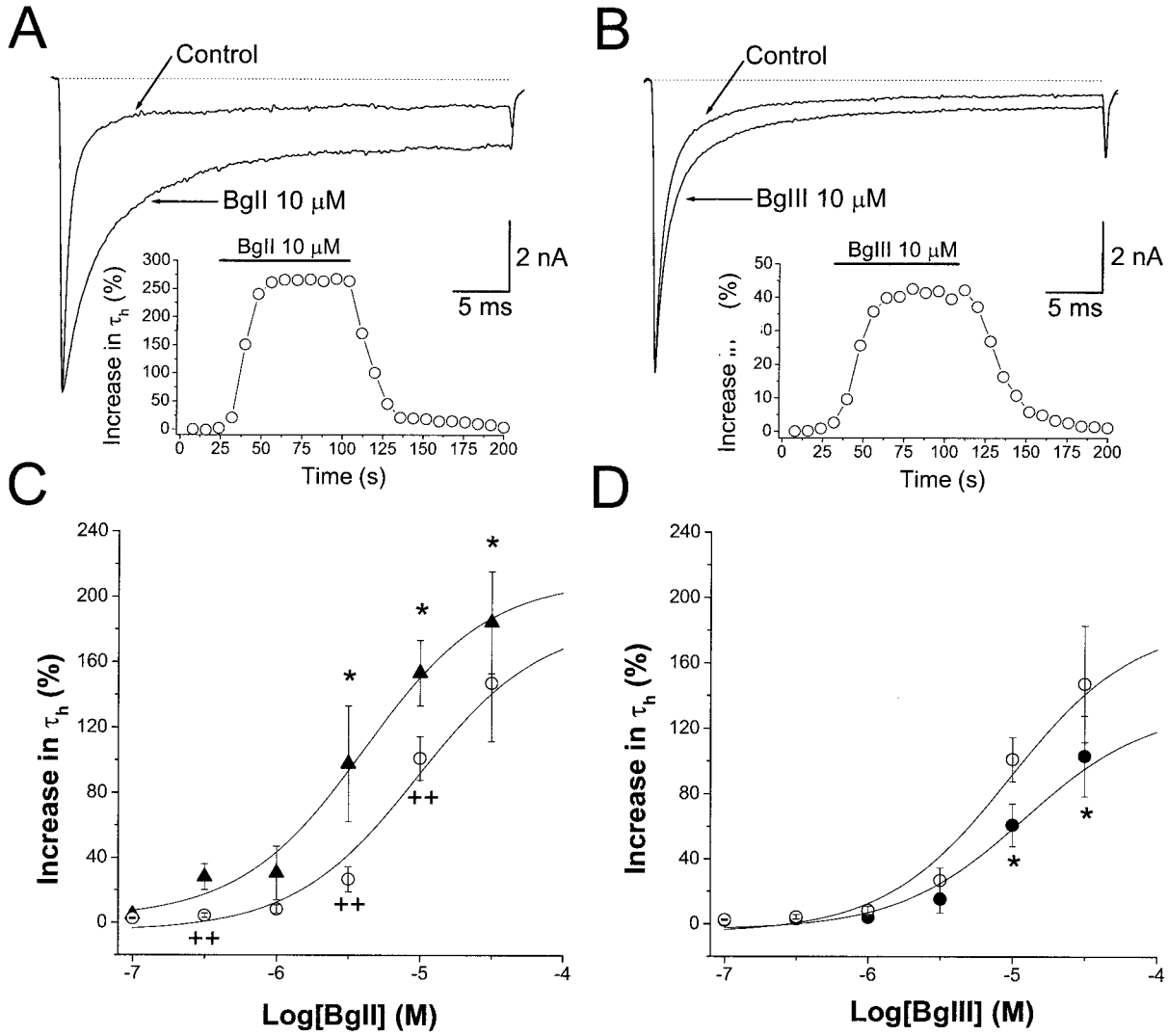

Fig. 2. Concentration-response curves of the effect of BgII, BgIII, and ATX-II. A and B, typical experiments showing the effects of 10 μM BgII and BgIII on TTX-S sodium currents, respectively. Traces were obtained by a single-step voltage protocol (40-ms depolarizing test pulses to −10 mV from a holding potential of −90 mV every 8 s). Toxins produced a marked slowing of the inactivation process. The insets show the time course of toxin effects on τ_h. Bars in the inserts indicate the time interval of toxin perfusion around the cell. C and D, concentration-response curves of the effect of ATX-II (n = 32; open circles), BgII (n = 87; triangles), and BgIII (n = 22; filled circles) on τ_h. Data were fit by (solid lines) the dose-response function described under *Materials and Methods*. The IC_{50} values calculated from these experiments were 4.1 ± 1.2 μM (BgII), 9.6 ± 1.3 (ATX-II), and 11.9 ± 1.4 μM (BgIII). Asterisks denotes a significant effect of BgII and BgIII with respect to its controls. ++ denotes significant effects with respect to ATX-II action (Student's t test; $p < 0.05$). Points represent the mean ± standard error of the mean.

characterized sea anemone toxin, an experimental series was done to study the effect of ATX-II on the DRG neurons (Fig. 2, C and D). ATX-II increased the inactivation time constant of the Na^+ TTX-S current with an IC_{50} value of 9.6 ± 1.3 μM, indicating that BgII is 2.3 more potent than ATX-II and 2.9 times more potent than BgIII in decreasing the τ_h of the Na^+ current. The maximum effect of both BgII and BgIII on the TTX-S sodium current inactivation time course was always achieved within the first minute after perfusion with either toxin, and once reached, it was stable throughout the exposure period to these agents (about 100 s). Washout of toxin effects was complete for both BgII and BgIII at 10 μM and took less than a minute (see inserts in Fig. 2). The slowing in the inactivation time course elicited by 10 μM BgII (n = 4) was voltage-dependent, whereas it was not for 10 μM BgIII (n = 4). Analysis of τ_h versus voltage curves showed that the effect of 10 μM BgII on the inactivation time constant of the TTX-S Na^+ current was significant ($p < 0.05$, Student's t test) only for voltages under −10 mV. The increase in τ_h induced by BgII at −10 mV was 64% smaller than that produced at −30 mV. At voltages above −10 mV, although there is a tendency of τ_h to increase, the change was not significant. The action of both toxins was not use-dependent (data not shown).

From current-voltage relationships, current density versus voltage curves were obtained by normalizing ionic current amplitudes as a function of membrane capacity (Fig. 3). Under control conditions, the maximum current density (−138 ± 24 pA/pF) was achieved at −10 mV. Perfusion with 10 μM BgII (Fig. 3A) produced a nonsignificant decrease ($p >$ 0.05, Student's t test) in the current density (−101 ± 12 pA/pF). Perfusion with BgIII (Fig. 3B) produced a nonsignificant increase in the current density. The reversal potential remained unchanged in the presence of toxins, and it was

consistent with the one calculated from the Nernst equation (18 mV).

The peak sodium conductance (G_{Na}) at several potential values was calculated as a chord conductance from the corresponding peak current. Normalized conductance curves were then fitted by a Boltzmann distribution and the corresponding $V_{1/2}$ and slope were calculated for each curve. Figure 4 shows the voltage dependence of G/G_{max} under control conditions and after perfusion with 10 μM of either BgII or BgIII. The mean value of $V_{1/2}$ for control experiments was -22 ± 0.8 mV. No significant differences ($p > 0.05$, Student's t test) in the G_{Na} were produced when BgII or BgIII were applied.

Measurements of the voltage dependence of h_∞ (steady-state inactivation parameter) were made using a two-pulse protocol. It was found that 10 μM of either BgII or BgIII caused a significant ($p < 0.05$, Student's t test) hyperpolarizing shift in the voltage at which half of the channels are inactivated ($V_{1/2\ inact}$), from a control value of -61 ± 0.8 mV to -73 ± 0.9 mV after BgII and -69 ± 1.4 mV after BgIII

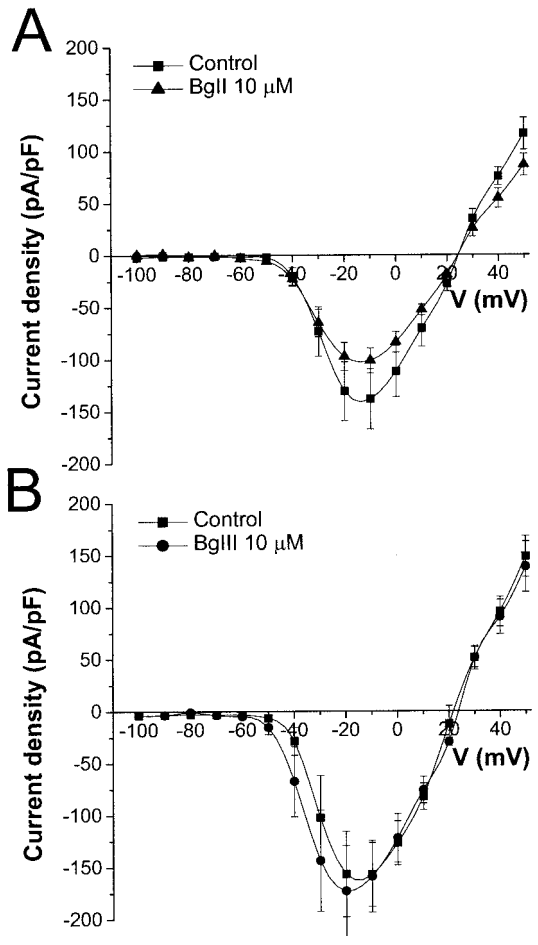

Fig. 3. Effects of BgII and BgIII on the current density versus voltage relationships. Curves were obtained by normalizing TTX-S current amplitudes to membrane capacity. Ionic currents were obtained by a voltage protocol in which 40-ms pulses between -100 and 70 mV were applied from a holding potential of -100 mV. Under control conditions ($n = 4$ for each case), the maximum current density was achieved at -10 mV. BgII (10 μM) (A; $n = 4$) produced a nonsignificant decrease in the current density at this voltage (-101 ± 12 pA/pF). When 10 μM BgIII (B; $n = 4$) was perfused, the maximum current density was larger (173 ± 44 pA/pF), although not significantly when compared with control values ($p > 0.05$; Student's t test).

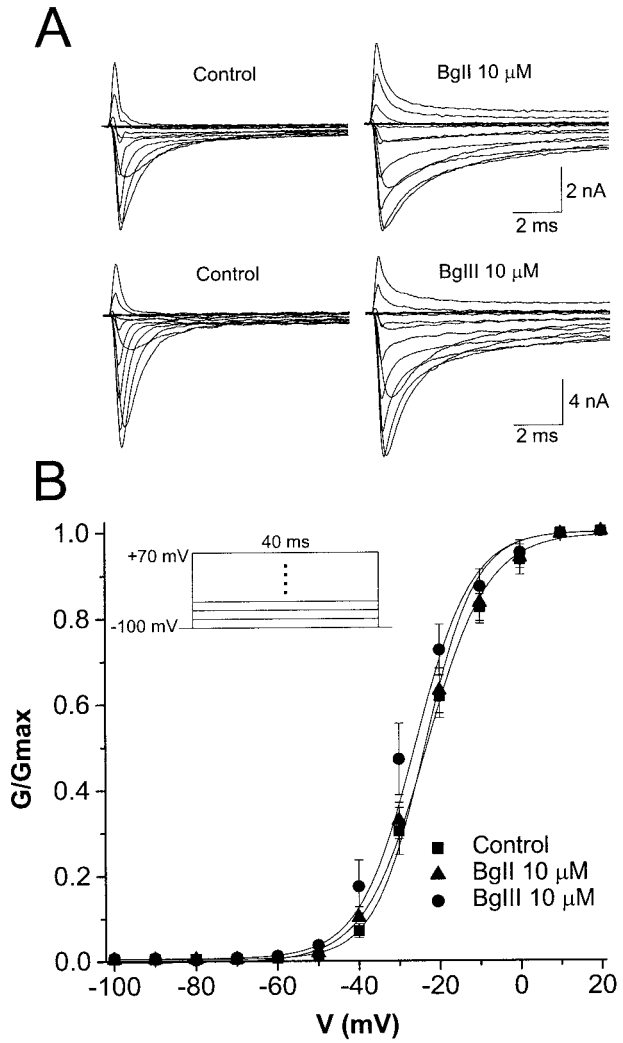

Fig. 4. Effects of BgII and BgIII on the voltage dependence of sodium conductance. A, typical experiments from which activation curves were obtained. B, the voltage dependence of G_{Na} under control conditions and after perfusion with BgII ($n = 4$) or BgIII ($n = 4$), each at a 10 μM concentration. Data were fit by a Boltzmann function (solid lines). The mean value of $V_{1/2}$ for control experiments was -22 ± 0.8 mV. After 10 μM BgII application, the $V_{1/2}$ was -24 ± 0.9 mV. After perfusion with 10 μM BgIII, the $V_{1/2}$ was -25 ± 1 mV. The slope for the three curves were also very similar, around 6.5 mV.

application (Fig. 5). The calculated slopes were 7.7 ± 0.6 mV (control), 8.8 ± 0.8 mV (BgII), and 10 ± 1.6 mV (BgIII). The slope of the curve for BgIII indicates that steady-state inactivation became significantly less voltage-dependent ($p < 0.05$, Student's t test). The hyperpolarization shift of the Na^+ current implies that at -70 mV the current availability in the presence of BgIII is 82% of the control and that in the presence of BgII it is 70% of the control value.

It has been shown that the recovery rate of the TTX-S current could be described by the sum of two exponential functions: a fast component (τ_f) with a time constant of a few milliseconds and a slow component (τ_s) with a time constant in the order of several hundred milliseconds. Elliot and Elliot (1993) pointed out the inherent difficulty in the characterization of the slow component, which would require the use of interpulse intervals lasting several seconds. For this reason, we defined τ_{hrec} as the time required to reach 63% of reactivated channels. Under control conditions, τ_{hrec} was 15.5 ± 2

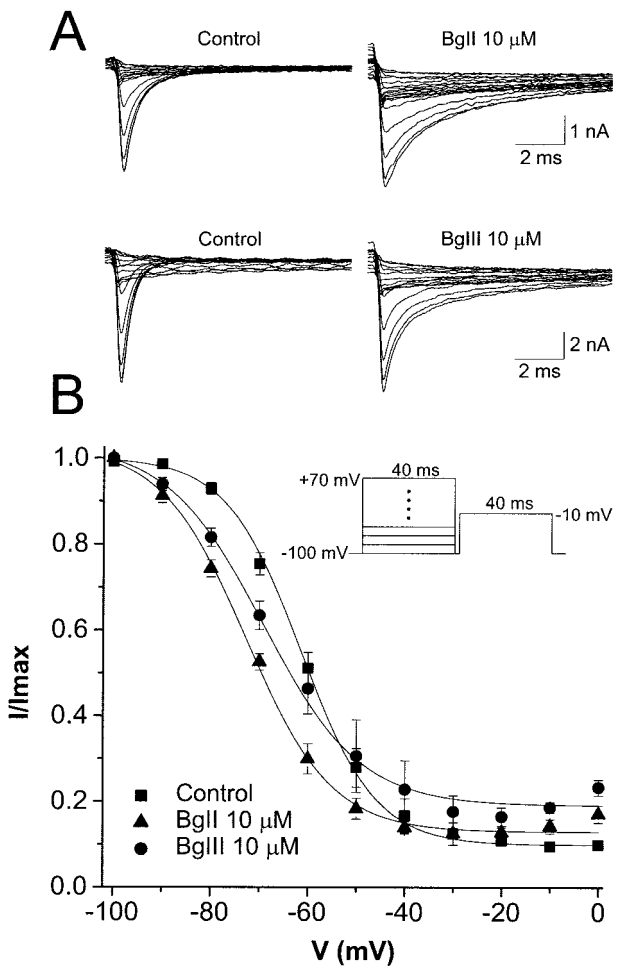

Fig. 5. Effects of BgII and BgIII on steady-state sodium current inactivation. A, typical records from which inactivation curves were obtained. B, steady-state inactivation profiles under control conditions ($n = 8$) and during perfusion of 10 μM BgII ($n = 4$) or 10 μM BgIII ($n = 4$). The steady-state inactivation (h_∞) was determined using the two-pulse protocol shown in the inset. Data were plotted as a function of the prepulse potential and fit by a Boltzmann function. A 10 μM concentration of either BgII or BgIII caused a significant hyperpolarizing shift in the $V_{1/2\ inact}$, from -61 ± 0.8 mV (control) to -73 ± 0.9 mV (BgII) and -69 ± 1.4 mV (BgIII).

ms. No significant effects ($p > 0.05$, Student's t test) were observed when 10 μM BgII ($n = 5$) or 10 μM BgIII ($n = 4$) were applied. The values of τ_{hrec} were 17.5 ± 1.2 and 16.4 ± 1.8 ms, respectively (data not shown).

Discussion

In the present work, we have made a comparative study of the effects of BgII, BgIII, and ATX-II on neuronal sodium currents. Our experiments show that the main effect exerted by both BgII and BgIII is a concentration-dependent slowing of the inactivation process of TTX-S sodium current, with no significant effects either on activation kinetics or current peak amplitude. No significant effects were observed on TTX-R sodium currents.

In our experimental conditions, BgII was about 3 times more potent than BgIII, a finding that is consistent with a previous study in mice by Loret et al. (1994), showing that BgII is more toxic than BgIII when injected intracerebroventricularly. These authors showed that the higher toxicity of BgII is correlated to a higher binding competition with the α-scorpion toxin AaH-II (from *Androctonus australis Hector*) in rat brain synaptosomes despite their lack of sequence homology. An interesting fact worth mentioning is that BgII and BgIII amino acid sequences are almost identical, differing only by a single amino acid; in BgIII, at position 16, an aspartic acid replaces the asparagine of BgII. BgII and BgIII exhibit a higher similarity with type 1 sea anemone toxins like ATX-II, ApA, or ApB (both from *Anthopleura xanthogrammica*) than with type 2 toxins like ShI (from *Stichodactyla helianthus*). The asparagine in position 16 is a very conservative residue among type 1 toxins. Our results reinforce the idea that this amino acid residue plays a central role in the action of these toxins (Loret et al., 1994; Goudet et al., 2001).

The electrophysiological effects of ATX-II and α-scorpion toxins on macroscopic TTX-S sodium currents include the inhibition of the Na^+ channel inactivation (Pelhate et al., 1984; Neumcke et al., 1985), the presence of sodium currents after prolonged depolarization (Warashina and Fujita, 1983), and voltage-dependent action (Strichartz and Wang, 1986). The effects of both BgII and BgIII are very similar. Nevertheless, only BgII showed a voltage-dependent action. As it was described for ATX-II, it seems to show more affinity for its binding site at hyperpolarized than at depolarized potentials (El-Sherif et al., 1992). In contrast, BgIII action was not voltage-dependent. According to Rogers et al. (1996), sea anemone toxin binding is less voltage-dependent than α-scorpion toxins, suggesting that they have fewer binding contacts outside of the IVS3-S4 loop, so it is subjected to less steric or torsional distortion when the channel is depolarized. The absence of voltage-dependent action observed for BgIII could be explained by a modification of the electrostatic interactions with the sodium channel due to the presence of an additional negative charge at the toxin molecule. In the literature, there are reports indicating a voltage-dependent action of ATX-II (Lawrence and Catterall, 1981; Strichartz and Wang, 1986) and α-PMTX (pompilidotoxin, a site 3 neurotoxin from wasp venom) (Sahara et al., 2000) and also a voltage-independent action (Vincent et al., 1980; Isenberg and Ravens, 1984). At the moment, there is not a clear explanation for these discrepancies, but it is possible that isoform or species-specific differences in gating among sodium channels could be playing a role in this respect. The fact that BgII and BgIII actions were not use-dependent suggests that these toxins show no preference for the open state of the sodium channel.

BgIII caused a decrease in the voltage dependence of sodium channel inactivation (i.e., significantly increased the slopes of steady-state inactivation). This result is in agreement with other studies involving site 3 neurotoxins (Gallagher and Bluementhal, 1994; Cahine et al., 1996; Chen et al., 2000).

In contrast with the lack of effect of BgII and BgIII on the TTX-R currents in DRG neurons, BgII produced a significant slowing of the inactivation and an increase in the slope of the inactivation curve in ventricular cardiomyocytes Na^+ currents that are TTX-R (Goudet et al., 2001). Moreover, according to our experiments, in the presence of BgII or BgIII, steady-state inactivation curves of DRG neurons showed a shift to the left (i.e., to more hyperpolarized potentials) in the voltage at which half of the channels are inactivated. This

effect is shared by several site 3 toxins (Gordon et al., 1996). BgII and BgIII applied on cloned hH1 sodium channels produced a depolarizing shift in the steady-state inactivation curves but no shift at all when tested on rat ventricular cardiomyocytes (Goudet et al., 2001). Neither BgII nor BgIII showed a significant effect on sodium current recovery from inactivation. These data are in agreement with the results reported by Goudet et al. (2001) in rat ventricular cardiomyocytes.

Several studies have revealed that sea anemone toxins bind with higher affinity to cardiac sodium channels than to neuronal ones (El-Sherif et al., 1992; Roden et al., 2002). The discrepancies between the actions of BgII and BgIII on cardiac and neuronal cells could be the result of tissue- or species-specific differences. TTX-R currents in DRG neurons are mainly due to type 1.8 and 1.9 Na^+ channels, whereas in the heart, the 1.5 subunit is mainly expressed (Novakovik et al., 2001; Dib-Hajj et al., 2002).

Site 3 sodium channel toxins have been suggested to slow the open state to inactivated state transition rate (Warashina and Fujita, 1983; Strichartz and Wang, 1986; Schreibmayer et al., 1987; Kirsch et al., 1989), but this phenomenon is difficult to study with macroscopic currents because current decay at a wide range of voltages represents a combination of delayed channel openings and channel inactivation (El-Sherif et al., 1992). Nevertheless, both the slowing of inactivation and the reduction in voltage dependence of steady-state inactivation observed in our experiments suggest that the general explanation proposed by Rogers et al. (1996) regarding the putative mechanism of action of site 3 toxins is also applicable to BgII and BgIII: 1) the toxin receptor site undergoes a conformational change that is required for fast inactivation; 2) bound toxin slows this conformational change and, as a consequence, slows the inactivation process; and 3) since site 3 neurotoxins bound across the IVS3-S4 extracellular loop of the sodium channel and that translocation of IVS4 segment may be required for the inactivation gate to close, anemone toxins could be slowing or blocking such translocation and thus hindering inactivation. Slowing of the inactivation, however, would increase current density, an effect that has not been observed in our experiments; thus we cannot exclude that BgII and BgIII may also produce some degree of channel occlusion.

The existence of several peptides from different species that bind site 3 of the Na^+ channel is relevant from an evolutionary point of view, indicating that this site is conserved among species, thus constituting a target for poisonous toxins to act. Additionally, the analysis of peptide sequences of toxins acting on this site may allow the identification of the elements of the sequence that are essential for binding to site 3 of the Na^+ channel. This could be of particular relevance in the case of BgII and BgIII, toxins that only differ by a single amino acid.

Acknowledgments

We are profoundly in debt to Professor Abel Aneiros for the kind gift of BgII and BgIII toxins and with Professor L. Beress for kindly supplying ATX-II. We are also grateful to M. Sánchez-Alvarez for proofreading the English version.

References

Adams ME and Olivera BM (1994) Neurotoxins: overview of an emerging research technology. *Trends Neurosci* **17:**151–155.

Alessandri-Haber N, Lecoq A, Gasparini S, Grangier-Macmath G, Jacquet G, Harvey AL, de Medeiros C, Rowan EG, Gola M, Ménez A, and Crest M (1999) Mapping the functional anatomy of BgK on Kv1.1, Kv1.2 and Kv1.3. Clues to design analogs with enhanced selectivity. *J Biol Chem* **274:**35653–35661.

Aneiros A, García I, Martínez JR, Harvey AL, Anderson AJ, Marshall DL, Engström Å, Hellman U, and Karlsson E (1993) A potassium channel toxin from the secretion of the sea anemone *Bunodosoma granulifera*. *Biochim Biophys Acta* **1157:**86–92.

Baker MD and Wood JN (2001) Involvement of Na^+ channels in pain pathways. *Trends Pharmacol Sci* **22:**27–31.

Bossu JL and Feltz A (1984) Patch-clamp study of the tetrodotoxin-resistant sodium current in group C sensory neurons. *Neurosci Lett* **51:**241–246.

Cahine M, Plante E, and Kallen RJ (1996) Sea anemone toxin ATX-II modulation of heart and skeletal muscle sodium channel α-subunits expressed in tsA201 cells. *J Membr Biol* **152:**39–48.

Catterall WA (1995) Structure and function of voltage-gated ion channels. *Annu Rev Biochem* **64:**493–531.

Catterall WA (2000) From ionic currents to molecular mechanisms: the structure and function of voltage-gated sodium channels. *Neuron* **26:**13–25.

Couroud F, Rochat H, and Lissitzky S (1978) Binding of scorpion and sea anemone toxins to a common site related to the action potential Na^+ ionophore in neuroblastoma cells. *Biochem Biophys Res Commun* **83:**1525–1530.

Chen H, Gordon D, and Heinemann SH (2000) Modulation of cloned skeletal muscle sodium channels by the scorpion toxins Lqh II, Lqh III and LqhαIT. *Pfluegers Arch* **439:**423–432.

Dauplais M, Lecoq A, Song J, Cotton J, Jamin N, Gilquin B, Roumestand CH, Vita C, de Medeiros CLC, Rowan EG, et al. (1997) On the convergent evolution of animal toxins. Conservation of a diad of functional residues in potassium channel-blocking toxins with unrelated structures. *J Biol Chem* **272:**4302–4309.

Dib-Hajj S, Black JA, Cummins TR, and Waxman SG (2002) NaN/Na v 1.9: a sodium channel with unique properties. *Trends Neurosci* **25:**253–259.

El-Sherif N, Fozzard HA, and Hanck DA (1992) Dose-dependent modulation of the cardiac sodium channel by sea anemone toxin ATXII. *Circ Res* **70:**285–301.

Elliot AA and Elliot JR (1993) Characterization of TTX-Sensitive and TTX-Resistant sodium currents in small cells from adult rat dorsal root ganglia. *J Physiol (London)* **463:**39–56.

Gallagher MJ and Bluementhal KM (1994) Importance of the unique cationic residues arginine 12 and lysine 49 in the activity of the cardiotonic polypeptide anthopleurin B. *J Biol Chem* **269:**254–259.

Garateix A, Vega R, Salceda E, Cebada J, Aneiros A, and Soto E (2000) BgK anemone toxin inhibits outward K^+ currents in snail neurons. *Brain Res* **864:**312–314.

Gordon D, Martin-Eauclaire MF, Castèle S, Kopeyan C, Carlier E, Khalifa RB, Pelhate M, and Rochat H (1996) Scorpion toxins affecting sodium current inactivation bind to distinct homologous receptor sites on rat brain and insect sodium channels. *J Biol Chem* **271:**8034–8045.

Gordon D, Savarin Ph, Gurevitz M, and Zinn-Justin S (1998) Functional anatomy of scorpion toxins affecting sodium channels. *J Toxicol-Toxin Rev* **17:**131–159.

Goudet C, Ferrer T, Galan L, Artiles A, Batista CFV, Possani LD, Alvarez J, Aneiros A, and Tytgat J (2001) Characterization of two *Bunodosoma granulifera* toxins active on cardiac sodium channels. *Br J Pharmacol* **134:**1195–1206.

Isenberg G and Ravens U (1984) The effects of *Anemonia sulcata* toxin (ATXII) on membrane currents of isolated mammalian myocytes. *J Physiol (London)* **357:**127–149.

Kirsch GE, Skattebol A, Possani LD, and Brown AM (1989) Modification of Na channel gating by an alpha scorpion toxin from *Tityus serrulatus*. *J Gen Physiol* **93:**67–83.

Lawrence JC and Catterall WA (1981) Tetrodotoxin-insensitive sodium channels. Binding of polypeptide neurotoxins in primary cultures of rat muscle cells. *Biochim Biophys Acta* **901:**273–282.

Loret EP, Menendez Soto del Valle R, Mansuelle P, Sampieri F, and Rochat H (1994) Positively charged amino acid residues located similarly in sea anemone and scorpion toxins. *J Biol Chem* **269:**16785–16788.

Narahashi T (1998) *Chem* modulation of sodium channels, in *Ion Channel Pharmacology* (Soria B and Ceña V eds) pp 23–73, Oxford University Press, New York.

Neumcke B, Schwarz W, and Stampfli R (1985) Comparison of the Anemonia toxin II on sodium and gating currents in frog myelinated nerve. *Biochim Biophys Acta* **814:**111–119.

Norton RS (1997) Anemone toxins (type II), in *Guidebook to Protein Toxins and Their Use in Cell Biology* (Rappuoli R and Montecucco C eds) pp 134–137, Oxford University Press, New York.

Novakovik SD, Eglen RM, and Hunter JC (2001) Regulation of Na^+ channel distribution in the nervous system. *Trends Neurosci* **24:**473–478.

Pelhate M, Laufer J, Pichon Y, and Zlotkin E (1984) Effects of several sea anemone and scorpion toxins on excitability and ionic currents in the giant axon of the cockroach. *J Physiol (Paris)* **79:**309–317.

Roden DM, Balser JR, George AL Jr, and Anderson ME (2002) Cardiac Ion Channels. *Annu Rev Physiol* **64:**431–475.

Rogers JC, Qu YS, Tanada TN, Scheuer T, and Catterall WA (1996) Molecular determinants of high affinity binding of α-scorpion toxin and sea anemone toxin in the S3–S4 extracellular loop in domain IV of the Na^+ channel subunit. *J Biol Chem* **271:**15950–15962.

Roy ML and Narahashi T (1992) Differential properties of tetrodotoxin-sensitive and tetrodotoxin-resistant sodium channels in rat dorsal root ganglion neurones. *J Neurosci* **12:**2104–2111.

Sahara Y, Gotoh M, Konno K, Miwa A, Tsubokawa H, Robinson HPC, and Kawai N (2000) A new class of neurotoxin from wasp venom slows inactivation of sodium current. *Eur J Neurosci* **12:**1961–1970.

Salinas EM, Cebada J, Valdes A, Garateix A, Aneiros A, and Alvarez JL (1997) Effects of a toxin from the mucus of the Caribbean sea anemone (*Bunodosoma granulifera*) on the ionic currents of single ventricular mammalian cardiomyocytes. *Toxicon* **35:**1699–1709.

Schreibmayer W, Kazerani H, and Tritthart H (1987) A mechanistic interpretation of the action of toxin II from *Anemonia sulcata* on the cardiac sodium channel. *Biochim Biophys Acta* **901:**273–282.

Strachan LC, Lewis RJ, and Nicholson GM (1999) Differential actions of Pacific ciguatoxin-1 on sodium channel subtypes in mammalian sensory neurons. *J Pharmacol Exp Ther* **288:**379–388.

Strichartz G, Rando T, and Wang GK (1987) An integrated view of the molecular toxinology of sodium channel gating in excitable cells. *Ann Rev Neurosci* **10:**237–267.

Strichartz GR and Wang GK (1986) Rapid voltage-dependent dissociation of scorpion alpha-toxins coupled to Na channel inactivation in amphibian myelinated nerves. *J Gen Physiol* **88:**413–435.

Trainer VL, Baden DG, and Catterall WA (1994) Identification of peptide components of the brevotoxin receptor site of rat brain sodium channels. *J Biol Chem* **269:**19904–19909.

Vincent JP, Balerna M, Barhanin J, Fosset M, and Lazdunski M (1980) Differential actions of Pacific ciguatoxin-1 on sodium channel subtypes in mammalian sensory neurons. *J Pharmacol Exp Ther* **288:**379–388.

Warashina A and Fujita S (1983) Effects of sea anemone toxins on the sodium inactivation process in crayfish axons. *J Gen Physiol* **81:**305–323.

Address correspondence to: Dr. Emilio Salceda, Instituto de Fisiología, Universidad Autónoma de Puebla, Apartado Postal 406, Puebla, Pue., CP 72001, México. E-mail: esalceda@siu.buap.mx